

Optimization of spin-torque switching using AC and DC pulses

Tom Dunn¹, and Alex Kamenev^{1,2}

¹Department of Physics, University of Minnesota, Minneapolis, Minnesota 55455, USA.

²Fine Theoretical Physics Institute, University of Minnesota, Minneapolis, Minnesota 55455, USA.

We explore spin-torque induced magnetic reversal in magnetic tunnel junctions using combined AC and DC spin-current pulses. Employing a macrospin model we calculate the optimal pulse times for both the AC and DC pulses, needed to minimize the Joule heat loss during the switching process for a given AC driving frequency and spin-current magnitude. The results of this optimization are compared against numeric simulations. Finally we show this optimization leads to different dynamic regimes, where switching is optimized by either a purely AC or DC spin-current, or a combination AC/DC spin-current, depending on the anisotropy energies and the spin-current polarization.

PACS numbers: 85.75.Dd, 85.75.-d, 75.75.Jn

The question of spin-torque (ST) efficiency in switching the free layer in magnetic tunnel junctions (MTJ) has been of great interest in recent years [1–3] due to the potential of spintronic memory as a universal non-volatile memory element [4, 5]. For co-linear MTJs, using DC current pulses, the most efficient prescription has been shown to be roughly twice the critical current [6, 7]. Recent experimental research, however, has shown perpendicularly polarized DC spin-current pulses can produce switching much faster and more efficient than in the co-linear case [8, 9]. Furthermore, previous theoretical work by the authors of this paper has shown perpendicularly polarized AC spin-currents can improve the efficiency further in MTJs with strong easy-plane anisotropy by inducing a resonant response in the free layer [10].

For MTJs with weak easy-plane anisotropy (such as those used in Ref. [11–13]) however, this purely AC method becomes less effective. This is a result of the magnetization spending more time at large azimuthal angle through the switching process where the perpendicular ST is weaker. Conversely, as the magnetization spends more time at large azimuthal angles the strength of the parallel DC ST increases. In fact, for some cases the strengths of the AC and DC ST may intersect allowing AC ST to dominate for low energy orbits and DC ST for high energy orbits. This tradeoff suggests an alternative means of magnetic switching in MTJs with weak easy-plane anisotropy. Instead of using a purely AC or DC spin-current, an AC pulse may be used to push the magnetization to a higher energy state, where a DC spin-current can then be used to switch the magnetization the rest of the way. Such an AC/DC current pulse strategy is considered experimentally in Ref. [14] and theoretically using micromagnetic simulations in Ref. [15] and shown to markedly improve the efficiency of the switching process.

In this paper provide a theoretical description of magnetic switching using such AC/DC spin-currents. This description is then use to determine the optimal AC and DC current pulse times which minimize the Joule heat loss during the switching process. Such switching is then optimized numerically with respect to spin-current

strength and AC drive frequency which is then compared to numeric simulations. The macrospin model employed is a simplification of the free layer dynamics. It is useful to provide intuition and approximate a semi-quantitative description of the switching kinetics. Good agreement between macrospin models and experimental results for AC and DC switching strategies are found in Ref. [14].

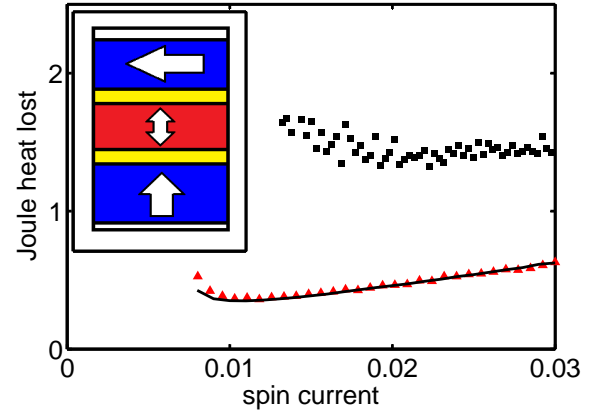


FIG. 1: (Color online) Simulated optimal Joule heat loss during switching process in arbitrary units as a function of spin current amplitude (I_s/M_s) for DC (black squares) and AC/DC (red triangles) spin current methods. Black line represents the theoretical optimal Joule heat loss. Here $\alpha = 0.015$, $H_z = 0.5M_s$, $H_x = 0$, $T_s^{AC} = T_s^{DC} = I_s$, $\mathbf{m}_p = -\hat{\mathbf{e}}_x - \hat{\mathbf{e}}_z$ and $T = 300K$. Inset shows diagram of MTJ. Blue and red regions represent fixed and free layers respectively. Yellow regions non-magnetic and current flows along vertical axis. Arrows indicate fixed layer polarizations and free layer easy axis.

To model the magnetic switching using this AC/DC strategy we treat the free layer as a single magnetic domain with a constant saturation magnetization M_s and magnetization direction specified by a time-dependent unit vector $\hat{\mathbf{m}}(t)$. Its dynamics is described by the Landau-Lifshitz-Gilbert equation [16] with Slonczewski spin torque term [17, 18]. Thermal noise is included

as a random contribution $\mathbf{h}(t)$ to the effective field $\mathbf{H}_{\text{eff}}(\mathbf{m}, t) \propto -\nabla_{\mathbf{m}} E(\mathbf{m})$ [19], with correlator given by the fluctuation-dissipation theorem [20]. Here E is the magnetic anisotropy energy

$$E(\mathbf{m}) = \frac{\mu_0 M_s}{2} \left[H_z \left(1 - (\mathbf{m} \cdot \hat{\mathbf{e}}_z)^2 \right) + H_x (\mathbf{m} \cdot \hat{\mathbf{e}}_x)^2 \right], \quad (1)$$

where μ_0 is the permeability of free space, $\hat{\mathbf{e}}_z$ and $\hat{\mathbf{e}}_x$ are the directions of the easy-axis and easy-plane respectively, and H_z and H_x are the strengths of the easy-axis and easy-plane anisotropy fields respectively. The height of the energy barrier between the two easy-axis directions is $E_b = \mu_0 H_z M_s / 2$.

The spin-current $\vec{I}_s(t)$ consists of two pulses. An AC pulse $\vec{I}_s^{AC} \sin(\omega t)$, followed immediately by a DC pulse \vec{I}_s^{DC} as shown in Fig. 2. These pulses are characterized by six parameters: the AC driving frequency ω , the AC and DC pulse durations, t_{AC} and t_{DC} , the AC and DC spin-current amplitudes, \mathcal{I}_s^{AC} and \mathcal{I}_s^{DC} (in units of magnetization), and the polarization vector \mathbf{m}_p such that $\vec{I}_s = \mathcal{I}_s \mathbf{m}_p$. A sample switching trajectory is shown in Fig. 2 for a free layer with uniaxial anisotropy.

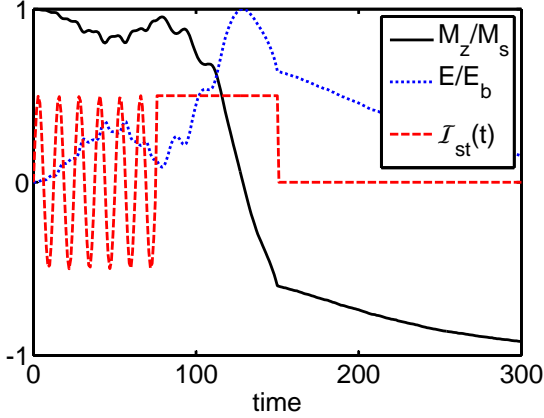


FIG. 2: (Color online) Simulated switching trajectory calculated via numeric integration of the LLG equation; M_z (black, solid) and energy E (blue, dotted) along with spin-current in arbitrary units (red, dashed). Here time is in units of $(\gamma M_s)^{-1}$, $\mathcal{I}_s^{AC} = \mathcal{I}_s^{DC} = 0.02 M_s$ and $\omega = \gamma H_z$ with other parameters the same as in Fig. 1.

As a specific example we performed numerical simulations of a free layer with uniaxial anisotropy, $H_z = 0.5 M_s$ and $H_x = 0$ (taken from Ref. [12]), and polarization vector $\mathbf{m}_p = -\hat{\mathbf{e}}_x - \hat{\mathbf{e}}_z$ (for schematic of MTJ see inset Fig. 1). For simplicity the AC and DC spin-current strengths are taken to be equal $\mathcal{I}_s = \mathcal{I}_s^{AC} = \mathcal{I}_s^{DC}$. The negative sign in the polarization vector is to ensure switching from the $+\hat{\mathbf{e}}_z$ to $-\hat{\mathbf{e}}_z$ energy minimum using positive DC current.

To determine the optimal switching protocol numerous trials were done for a range of spin-current amplitudes, frequencies, and AC/DC pulse times. Each trial

consisted of 10^3 simulated switching events. The energy lost to Joule heat is $J = \int_0^{t_{\text{total}}} R(\mathbf{m}) \mathcal{I}_s^2(t) dt$ where $t_{\text{total}} = t_{AC} + t_{DC}$ is the total pulse time and $R(\mathbf{m})$ is a resistance that depends on the magnetization direction. In practice this resistance varies little through the switching process [21, 22] thus the Joule heat may be approximated as

$$J \propto (\mathcal{I}_s^{DC})^2 t_{DC} + (\mathcal{I}_s^{AC})^2 \frac{t_{AC}}{2}. \quad (2)$$

The parameter set resulting in the least Joule heat loss, with switching probability above 99.5%, for each spin-current amplitude \mathcal{I}_s is shown in Fig. 1. Notice the optimal energy loss using this AC/DC method is almost a third of the purely DC method for the same device and the optimal current is roughly half.

To understand this optimal AC/DC protocol it is first convenient to describe the LLG equation, in terms of the locally orthogonal coordinates of energy E and angle φ [16, 23]. For spin-currents that are not too large (i.e. on order of the DC critical switching current) E is a slow variable relative to φ , see Fig. 2. This separation of time scales allows the equation of motion for E to be averaged over each Stoner-Wohlfarth (SW) orbit [16, 24, 25]. For DC spin-currents this reduces the LLG equation in the initial potential well to

$$\dot{E} = -\alpha U(E) + \mathcal{I}_s^z V_{DC}(E), \quad (3)$$

where α is the dimensionless Gilbert damping constant and $\mathcal{I}_s^z = \mathcal{I}_s^{DC} \mathbf{m}_p \cdot (-\hat{\mathbf{e}}_z)$ is the portion of the DC spin-current polarized along the easy-axis, $-\hat{\mathbf{e}}_z$ direction. For the uniaxial case the generalized forces, averaged over the SW orbit with energy E , are given by

$$\begin{aligned} U(E) &= \gamma 4E(E_b - E)/M_s, \\ V_{DC}(E) &= \gamma 2E(1 - E/E_b)^{1/2}, \end{aligned} \quad (4)$$

and correspond to the effects of damping and DC ST respectively.

For AC spin-currents, with driving frequency ω close to the natural frequency of the free layer, the magnetization tends to precess with the driving frequency ω [26, 27]. As a result the precessional dynamics can be expressed in terms of a relative phase $\phi(t) = \varphi(t) - \omega t$ which is also slow varying relative to φ . Thus the same averaging procedure used in the DC case may be applied to both E and ϕ equations of motion [10, 16], along with the relation $\sin(\omega t) = \sin(\varphi - \phi)$ to single out terms even and odd in φ , giving

$$\begin{aligned} \dot{E} &= -\alpha U(E) - \mathcal{I}_s^x V_{AC}(E) \sin \phi, \\ \dot{\phi} &= \Omega(E) - \omega - \mathcal{I}_s^x W(E) \cos \phi, \end{aligned} \quad (5)$$

in the initial potential well. Here $\Omega(E)$ is the natural frequency of the free layer about the SW orbit with energy E , and $\mathcal{I}_s^x = \mathcal{I}_s^{AC} \mathbf{m}_p \cdot (-\hat{\mathbf{e}}_x)$ is the portion of the AC spin-current polarized along the easy-plane axis, $-\hat{\mathbf{e}}_x$ direction.

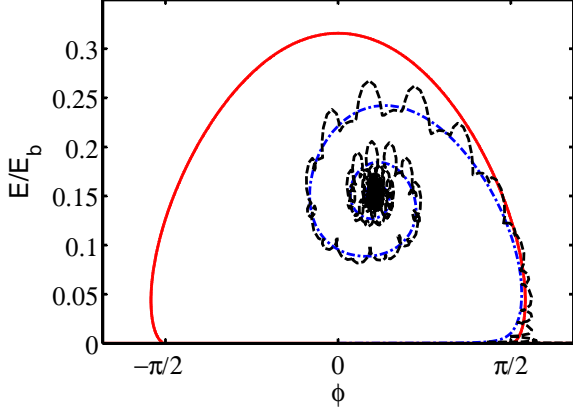


FIG. 3: (Color online) Simulated energy E vs phase ϕ (black,dashed) calculated via numerical integration of the LLG equation, average energy and phase (red,dot-dashed) calculated from integration of Eqn. (5), and $\mathcal{H} = 0$ trajectory (blue,solid) from Eqn. (7). Same parameters as Fig. 2.

For the uniaxial case $\Omega(E) = \gamma H_z (1 - E/E_b)^{1/2}$ and the two new generalized forces are given by

$$\begin{aligned} V_{AC}(E) &= \gamma(E - E_b)(E/E_b)^{1/2}, \\ W(E) &= \gamma(E_b/4E)^{1/2}, \end{aligned} \quad (6)$$

which correspond to the effects of the AC ST on the energy and precessional motion respectively. A sample trajectory for E and ϕ simulated using the LLG equation is shown in Fig. 3 along with the trajectory given by Eqs. (5). Notice the energy first overshoots the equilibrium energy before winding down to it.

Setting the LHS of Eqs. (5) to zero give the equilibrium energy and phase. The equilibrium energy E_{eq} for the uniaxial case is shown in Fig. 4 along with simulated values. The hysteresis curve formed is in good qualitative agreement with experimental and macrospin results in Ref. [26, 28]. The simulations show two *jump frequencies* at ω_1 and ω_2 where the energy abruptly jumps between the upper and lower branches. Since the initial energy is near zero for any switching process, for $\omega < \omega_2$ the trajectory will overshoot and then relax to the lower equilibrium branch while for $\omega > \omega_2$ the trajectory will overshoot and then relax to the upper. As a result $\omega_2 \lesssim \omega$ produces the largest overshoot energies.

In the absence of damping, $\alpha = 0$, the trajectories given by Eqs. (5) possess an integral of motion and can thus be described as lines of constant value for some function $\mathcal{H}(E, \phi)$ [10, 16]. For the uniaxial case

$$\begin{aligned} \mathcal{H}(E, \phi) &= 2\omega \left(1 - \sqrt{\frac{E_b}{E_b - E}} \right) - \gamma \mathcal{I}_s \sqrt{\frac{E}{E_b - E}} \cos \phi \\ &\quad - \gamma H_z \ln \left(1 - \frac{E}{E_b} \right). \end{aligned} \quad (7)$$

A sample trajectory for zero initial energy, $\mathcal{H}(E, \phi) = 0$, is shown in Fig. 3. Notice the simulated trajectory from the LLG equation and the trajectory calculated from Eqs. (5) closely follow the $\mathcal{H} = 0$ trajectory making it a good zeroth order approximation for weak damping, $\alpha \ll 1$.

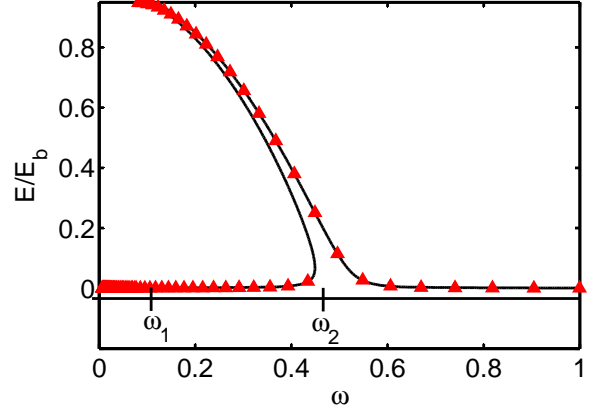


FIG. 4: (Color online) Equilibrium energy as a function of frequency found via numeric integration of the LLG equation (red,triangles) and calculated from Eqn. (5). Same parameters as in Fig. 2.

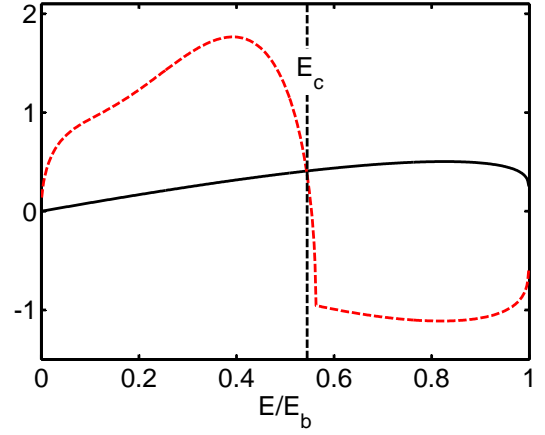


FIG. 5: (Color online) Plots \dot{E}_{AC} (red,dashed) and $2\dot{E}_{DC}$ (black,solid) in arbitrary units for parameters $H_x = M_s$, $H_z = 0.25M_s$, $\alpha = 0.015$, $\mathcal{I}_s^x = \mathcal{I}_s^z = 0.02M_s$, $\mathbf{m}_p = -\hat{\mathbf{e}}_x - \hat{\mathbf{e}}_z$ and $\omega = \gamma 2H_z$.

Using Eqs. (16), (5) and (7) the energy trajectory for any AC/DC spin-current can be calculated. However, the question of when to go from an AC to a DC spin-current is still of critical importance. To solve this we look for the combination of AC and DC pulse times which minimize the Joule heat loss for a given set of parameters. These pulse times may be calculated using Eqs. (16) and (5) as

$$t_{AC} = \int_0^{E_c} \frac{dE}{\dot{E}_{AC}}, \quad t_{DC} = \int_{E_c}^{E_b} \frac{dE}{\dot{E}_{DC}}, \quad (8)$$

where the ϕ dependence in \dot{E}_{AC} is eliminated using Eqn. (7), and E_c is the energy where the spin-current goes from AC to DC. In this description the optimal pulse times are found by solving $\frac{\partial J}{\partial E_c} = 0$. Substituting Eqs. (8) into Eqn. (2) and taking the derivative with respect to E_c gives the optimization criteria

$$\frac{\dot{E}_{DC}(E_c)}{(\mathcal{I}_s^{DC})^2} = 2 \frac{\dot{E}_{AC}(E_c)}{(\mathcal{I}_s^{AC})^2}. \quad (9)$$

Thus the optimal strategy when $\mathcal{I}_s^{AC} = \mathcal{I}_s^{DC}$ is to use an AC spin-current until the DC energy current is twice the AC energy current. An example of this realization is shown in Fig. 5. It should be noted that Eqn. (9) may have more than one solution. Thus care must be taken to ensure the E_c used is indeed the global minimum.

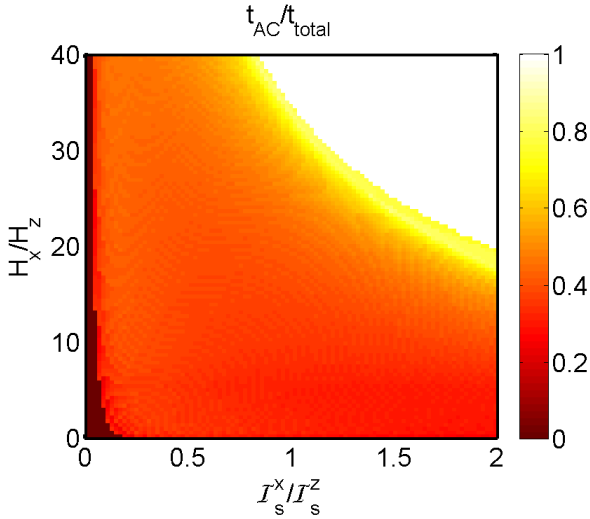


FIG. 6: (Color online) Shows t_{AC}/t_{total} for a range of H_x/H_z and I_s^x/I_s^z . Here $H_z = 0.5M_s$, $\alpha = 0.015$, $\omega = \Omega(0)$ and $\mathcal{I}_z = 2\mathcal{I}_c$ where \mathcal{I}_c is the DC critical current.

Using Eqs. (8) (9) the Joule heat loss can be calculated as a function of spin-current and frequency $J(\mathcal{I}_s^{AC}, \mathcal{I}_s^{DC}, \omega)$. The frequency ω that gives most efficient switching protocol does not lend itself to a simple analytic solution, however determining it numerically is relatively simple. The Joule heat loss using this optimal frequency is shown in Fig. 1 as a function of spin-current along with simulations of the LLG equation, optimized numerically for a uniaxial free layer. From simulations and the analysis described here, we found the optimal frequency to be slightly larger than the upper bifurcation frequency ω_2 .

The optimization method for this AC/DC method outlined above is not limited to the uniaxial case shown here. It can be applied much more generally allowing an optimal AC/DC spin-current protocol to be determined for any free layer with easy-axis and easy-plane anisotropy, see supplemental material [16]. To illustrate the range of possible strategies that may optimize this

AC/DC method Fig. 6 shows the optimal AC pulse time as a fraction of the total pulse time t_{AC}/t_{total} , for a broad range of anisotropy configurations H_x/H_z and spin-current polarizations ratios $\mathcal{I}_s^x/\mathcal{I}_s^z$. Here t_{AC}/t_{total} is calculated numerically using Eqs. (9) (8) for AC frequency $\omega = \Omega(0)$ and $\mathcal{I}_s^{AC} = \mathcal{I}_s^{DC} = 2\mathcal{I}_c$ where \mathcal{I}_c is the DC critical current. One can see there is a large region where purely AC spin-current pulses are more energy efficient than purely DC pulses ($t_{AC}/t_{total} = 1$), as well as a broad a broad region where the optimal strategy uses combined AC/DC spin-currents, ($0 < t_{AC}/t_{total} < 1$). There is also a narrow range where DC spin-currents are optimal ($t_{AC}/t_{total} = 0$). This range of results stresses there is no single general optimal application of either AC, DC, or combined AC/DC current pulses for MTJs. Instead the optimal strategy for each MTJ must be determined carefully as outlined above.

In conclusion we have developed a theoretical description for magnetic switching using consecutive AC and DC spin-current pulses as well as a means for minimizing the Joule heat loss associated with such strategies. It provides a means of determining the optimal AC and DC pulse durations, t_{AC} and t_{DC} , as well as the optimal AC driving frequency $\omega_2 \lesssim \omega_{opt}$ and spin-current strength. Such optimized strategies may use currents well below the DC critical current and result in significantly less Joule heat loss than purely DC or AC spin-current methods.

This work was supported by NSF Grant DMR-0804266 and U.S.-Israel Binational Science Foundation Grant 2008075.

Appendix - Supplemental material

The motion of the magnetic unit vector $\hat{\mathbf{m}}(t)$ is described by the Landau-Lifshitz Gilbert equation with Slonczewski spin torque term

$$\frac{d\hat{\mathbf{m}}}{dt} = \mathbf{\Gamma}_{LL} + \mathbf{\Gamma}_{GD} + \mathbf{\Gamma}_{Slon}, \quad (10)$$

where

$$\begin{aligned} \mathbf{\Gamma}_{LL} &= -\gamma \hat{\mathbf{m}} \times \mathbf{H}_{eff}, \\ \mathbf{\Gamma}_{GD} &= -\gamma \alpha \hat{\mathbf{m}} \times [\hat{\mathbf{m}} \times \mathbf{H}_{eff}], \\ \mathbf{\Gamma}_{Slon} &= -\gamma \mathcal{I}_s(t) \hat{\mathbf{m}} \times [\hat{\mathbf{m}} \times \mathbf{m}_p]. \end{aligned} \quad (11)$$

are the conservative Landau-Lifshitz torque, Gilbert damping torque, and Slonczewski torque respectively. The magnetization can also be described by the coordinates energy E and angle φ . The angle φ is the time into the orbit with energy E in the absence of spin-torque and damping, normalized to 2π and calculated from

$$dt = \frac{\mathbf{\Gamma}_{LL} \cdot d\hat{\mathbf{m}}}{|\mathbf{\Gamma}_{LL}|^2} = \frac{d\varphi}{\Omega(E)}, \quad (12)$$

where $\Omega(E)$ is the precessional frequency of the orbit with energy E such that $\oint dt = 2\pi/\Omega(E)$. Throughout

this appendix φ is taken to be zero along the easy-plane axis, $\hat{\mathbf{e}}_x$.

The magnetization $\hat{\mathbf{m}}(E, \varphi)$ is related to E and φ by the partial derivatives

$$\partial_\varphi \hat{\mathbf{m}} = \frac{\mathbf{\Gamma}_{LL}}{M_s \Omega(E)}; \quad \partial_E \hat{\mathbf{m}} = \gamma \frac{\hat{\mathbf{m}} \times \mathbf{\Gamma}_{LL}}{|\mathbf{\Gamma}_{LL}|^2}. \quad (13)$$

The unit vectors $\hat{\mathbf{E}}$ and $\hat{\varphi}$ are locally orthogonal, $\partial_\varphi \hat{\mathbf{m}} \cdot \partial_E \hat{\mathbf{m}} = 0$, thus the LLG equation may be written as $d\hat{\mathbf{m}}/dt = \partial_\varphi \hat{\mathbf{m}} \dot{\varphi} + \partial_E \hat{\mathbf{m}} \dot{E}$. Separating the energy and angle equations of motion gives

$$\dot{E} = -\mathbf{H}_{\text{eff}} \cdot (\mathbf{\Gamma}_{GD} + \mathbf{\Gamma}_{\text{Slon}}); \quad (14)$$

$$\dot{\varphi} = \Omega(E) - \Omega(E) \frac{\mathbf{\Gamma}_{LL} \cdot \mathbf{\Gamma}_{\text{Slon}}}{|\mathbf{\Gamma}_{LL}|^2}. \quad (15)$$

Averaging Eqs. (14) and (15) about φ for DC spin-currents gives

$$\begin{aligned} \dot{E} &= -\alpha U(E) + \mathcal{I}_s V_{DC}(E), \\ \dot{\varphi} &= \Omega(E) \end{aligned} \quad (16)$$

where

$$\begin{aligned} U(E) &= \frac{\Omega(E)}{2\pi M_s} \oint [d\mathbf{M} \times \mathbf{H}_{\text{eff}}] \cdot \mathbf{M}, \\ V_{DC}(E) &= \frac{\Omega(E)}{2\pi M_s} \oint [d\mathbf{M} \times \mathbf{M}] \cdot \mathbf{m}_p. \end{aligned} \quad (17)$$

Here the contour integrals follow orbits of constant energy.

For AC spin currents this averaging gives

$$\begin{aligned} \dot{E} &= -\alpha U(E) - \mathcal{I}_s V_{AC}(E) \sin \phi, \\ \dot{\phi} &= \Omega(E) - \omega - \mathcal{I}_s W(E) \cos \phi, \end{aligned} \quad (18)$$

where $\dot{\phi} = \dot{\varphi} - \omega$ and

$$V_{AC}(E) = \frac{\Omega(E)}{2\pi M_s} \oint [d\mathbf{M} \times \mathbf{M}] \cdot \mathbf{m}_p \cos \varphi, \quad (19)$$

$$W(E) = \gamma \frac{\Omega(E)^2}{2\pi M_s} \oint \frac{(d\mathbf{M} \cdot \mathbf{\Gamma}_{LL})(\mathbf{\Gamma}_{LL} \cdot \mathbf{m}_p)}{|\mathbf{\Gamma}_{LL}|^4} \sin \varphi. \quad (20)$$

Here again the contour integrals follow orbits of constant energy.

In the absence of damping $\alpha = 0$ Eqs. (18) follow lines of constant value $\mathcal{H}(E, \phi)$ given by

$$\mathcal{H}(E, \phi) = \int_0^E dE' \mathcal{J}(E') \left[\omega - \Omega(E') + \mathcal{I}_s W(E') \cos \phi \right] \quad (21)$$

where $\mathcal{J}(E)$ is the solution to the linear differential equation

$$V(E) \frac{d\mathcal{J}(E)}{dE} = \mathcal{J}(E) \left(W(E) - \frac{dV(E)}{dE} \right). \quad (22)$$

-
- [1] D. E. Nikonov, G. I. Bourianoff, G. Rowlands, and I. N. Krivorotov, *J. Appl. Phys.* **107**, 113910 (2010).
 - [2] L. Fricke, S. Serrano-Guisan, and H. W. Schumacher, *Physica B: Condensed Matter* **407**, 1153 (2012).
 - [3] S.-M. Seo and K.-J. Lee, *Appl. Phys. Lett.* **101**, 062408 (2012).
 - [4] S. Yuasa and D. D. Djayaprawira, *J. Phys. D: Appl. Phys.* **40**, R337 (2007).
 - [5] S. Matsunaga, K. Hiyama, A. Matsumoto, S. Ikeda, H. Hasegawa, K. Miura, J. Hayakawa, T. Endoh, H. Ohno, and T. Hanyu, *Applied Physics Express* **2**, 023004 (2009).
 - [6] D. Bedau, H. Liu, J.-J. Bouzaglou, A. D. Kent, J. Z. Sun, J. A. Katine, E. E. Fullerton, and S. Mangin, *Appl. Phys. Lett.* **96**, 022514 (2010).
 - [7] J. Swiebodzinski, A. Chudnovskiy, T. Dunn, and A. Kamenev, *Phys. Rev. B* **82**, 144404 (2010).
 - [8] A. D. Kent, B. zyilmaz, and E. del Barco, *Appl. Phys. Lett.* **84**, 3897 (2004).
 - [9] G. E. Rowlands, T. Rahman, J. A. Katine, J. Langer, A. Lyle, H. Zhao, J. G. Alzate, A. A. Kovalev, Y. Tserkovnyak, Z. M. Zeng, et al., *Appl. Phys. Lett.* **98**, 102509 (2011).
 - [10] T. Dunn and A. Kamenev, *J. Appl. Phys.* **112**, 103906 (2012).
 - [11] P. K. Amiri, Z. M. Zeng, J. Langer, H. Zhao, G. Rowlands, Y.-J. Chen, I. N. Krivorotov, J.-P. Wang, H. W. Jiang, J. A. Katine, et al., *Appl. Phys. Lett.* **98**, 112507 (2011).
 - [12] D. C. Worledge, G. Hu, D. W. Abraham, J. Z. Sun, P. L. Trouilloud, J. Nowak, S. Brown, M. C. Gaidis, E. J. OSullivan, and R. P. Robertazz, *Appl. Phys. Lett.* **98**, 022501 (2011).
 - [13] H. Zhao, B. Glass, P. K. Amiri, A. Lyle, Y. Zhang, Y.-J. Chen, G. Rowlands, P. Upadhyaya, Z. Zeng, J. A. Katine, et al., *J. Phys. D: Appl. Phys.* **45**, 025001 (2012).
 - [14] Y. T. Cui, J. C. Sankey, C. Wang, K. V. Thadani, Z. P. Li, R. A. Buhrman, and D. C. Ralph, *Phys. Rev. B* **77**, 214440 (2008).
 - [15] M. Carpentieri, M. Ricci, P. Burrascano, L. Torres, and G. Finocchio, *J. Appl. Phys.* **111**, 07C909 (2012).
 - [16] See Appendix for a more detailed formulation.
 - [17] J. C. Slonczewski, *J. Magn. Magn. Mater.* **159**, L1 (1996).
 - [18] L. Berger, *Phys. Rev. B* **54**, 9353 (1996).
 - [19] W. F. Brown, *Phys. Rev.* **130**, 1677 (1963).
 - [20] Non-equilibrium noise such as spin shot noise is omitted here as it is usually weaker than the thermal noise at room temperature [7].
 - [21] I. N. Krivorotov, N. C. Emley, J. C. Sankey, S. I. Kiselev, D. C. Ralph, and R. A. Buhrman, *Science* **307**, 228 (2005).
 - [22] Y.-T. Cui, G. Finocchio, C. Wang, J. A. Katine, R. A. Buhrman, and D. C. Ralph, *Phys. Rev. Lett.* **104**, 097201 (2010).
 - [23] T. Dunn, A. Chudnovskiy, and A. Kamenev, in *Fluctuating Nonlinear Oscillators* (2012), pp. 142–164.
 - [24] D. M. Apalkov and P. B. Visscher, *Phys. Rev. B* **72**,

- 180405(R) (2005).
- [25] T. Dunn and A. Kamenev, Appl. Phys. Lett. **98**, 143109 (2011).
- [26] J. C. Sankey, P. M. Braganca, A. G. F. Garcia, I. N. Krivorotov, R. A. Buhrman, and D. C. Ralph, Phys. Rev. Lett **96**, 227601 (2006).
- [27] W. Chen, J.-M. L. Beaujour, G. de Loubens, A. D. Kent, and J. Z. Sun, Appl. Phys. Lett. **92**, 012507 (2008).
- [28] W. Chen, G. de Loubens, J.-M. L. Beaujour, J. Z. Sun, and A. D. Kent, Appl. Phys. Lett. **95**, 172513 (2009).